Properties of Adsorbed Water Layers and the Effect of Adsorbed Layers on Interparticle Forces by Liquid Bridging

E. J. W. Wensink[†] and A. C. Hoffmann*

Department of Chemical Engineering, University of Groningen, Nijenborgh 4, 9747 AG Groningen, The Netherlands

M. E. F. Apol[‡] and H. J. C. Berendsen

Department of Biophysical Chemistry, University of Groningen, Nijenborgh 4, 9747 AG Groningen, The Netherlands

Received January 4, 2000. In Final Form: June 1, 2000

The potential of molecular dynamics (MD) simulation for the study and prediction of particle/particle and particle/wall interaction in the wide context of technology has been explored. The present study concerns the nature of adsorbed water and its effect on the interaction between two surfaces. Computer models of two opposing (1,0,−1) crystal surfaces of α-quartz (dimensions 5.49 × 4.91 nm) were constructed and up to 1500 water molecules positioned between the surfaces. The simulations were performed in the NVT ensemble in "math mode" at a temperature of 300 K. The axial profiles of density and mobility (the latter resolved in planar and axial components) in the adsorbed layers were studied. The separation between the crystal surfaces was varied, monitoring the adsorbed layer morphology and the forces acting on the crystals. Most of the simulations shown are with 1500 molecules between the plates, giving around 3.1 adsorbed monolayers, corresponding to a relative saturation (humidity) of 67% according to the BET isotherm. The density profiles show an ordered packing of molecules in the first two adsorbed layers with density peaks considerably higher than in bulk water and a low molecular mobility. The density tails off to zero, and the mobility rises to above that of bulk water at the surface of the adsorbed layer, which was clearly defined but undulating. Determination of the forces acting on the crystals was difficult due to strong fluctuations on a short time scale, so only simulations for long times yielded statistically significant average forces. At a surface separation of 3 nm, spontaneous bridge forming took place, paired with significant attractive forces between the crystals. The nature of the bridge is discussed. The observed bridging and resulting surface/surface force are shown to be roughly consistent with expectations based on macroscopic theory represented by the BET isotherm, the Kelvin equation (using the surface tension of bulk water), and a bridging force calculated from pressure-deficiency and surface tension contributions.

Introduction

The physical characteristics of particulate materials, such as flow properties, fluidizability, and mixing and segregation characteristics, belong to the most urgent research topics in the processing technology today. While we have a good understanding of the dynamics of fluids, the behavior of particulate materials, which is related not only to the characteristics of the constituent particles but also to the environmental conditions and the history of the material, is an altogether more complex problem. It is a well-known fact that factories processing particulate materials, as a consequence of our lack of fundamental understanding of their behavior, on the average operate much further below their design capacity than is true for the processing industry as a whole. Add to this that a very substantial part of the raw materials and intermediate and final products in the processing industry is in the form of particulates (e.g. powdered coal, catalysts, dry pigments, cement constituents, pharmaceutical powders, ground food stuffs, powders in the mining industry).

The physical behavior of particulates is determined by particle/particle and particle/wall interactions. Fluidizability, discharge from storage vessels, pneumatic conveyability, and tendency for caking on equipment walls are examples. In most practical cases these interactions are strongly influenced by impurities on the particle or wall surface or by adsorbed species, the nature of which depends on the processing environment. Under ambient conditions the most important adsorbate will often be moisture. Under normal room conditions, such as a relative humidity in the region 40−60%, two or three adsorbed monolayers will often be present on particles, dominating the interactions and therefore the physical characteristics of the material.

Figure 1 is a sketch of a particle/particle contact point with an adsorbate present. Powders of industrial importance have mean particle diameters ranging from a few micrometers to a few millimeters, but particles may be down to submicrometer size. Contact points will normally be between asperities on the surface, and the radius of curvature of these may be down to the nanometer range, depending on the material and the particle formation process. At present not enough information about the morphology of particle and wall surfaces on a nanometer scale is available. If there is no net external force acting on the contact region, part of the contact area will be in compression and part in tension as indicated. Strong pressures are involved, with possible elastic and/or plastic deformation of the solid. The presence of the adsorbate will influence the particle/particle interaction both by

[†] Current address: Department of Applied Physics, R-V5032, Chalmers University of Technology and Göteborg University, S-412 96 Göteborg, Sweden.

[‡] Current address: Department of Chemistry, University of Rome "La Sapienza", P. le A. Moro 5, 00185 Rome, Italy.

10.1021/la000009e CCC: $19.00
Published on Web 08/19/2000

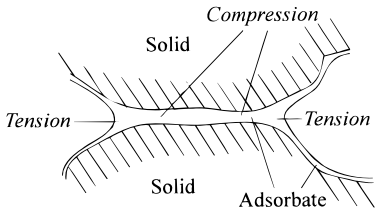

Figure 1. Sketch of a particle/particle contact point.

modifying the interaction between the molecules in the two particles but also by surface tension effects, such as possible bridge forming at the edge. If the adsorbent is porous, it can adsorb more material, since much adsorbate will concentrate in the pores. However, in most cases this does not change the problem of the particle/particle or particle/wall contact points.

The influence of adsorbed moisture on particle/particle and particle/wall interactions at high humidities is fairly well established through the macroscopic theory of liquid bridging (see below). At low or moderate humidities, however, or, more generally, under process conditions where just a few adsorbed monolayers are present, the picture is less clear and a number of unanswered questions remain. The whole problem of particle/particle and particle/wall interactions is of great importance to the engineering community, and the technique of molecular dynamics (MD) simulation has not yet been applied to the study of this issue. The object of the present work is to take a first look at the potential of molecular dynamics simulation techniques to study the influence of adsorbed species on particle/particle and particle/wall interactions in general.

Macroscopic Theories for Adsorption and Its Effect on Interparticle Forces. The number of monolayers of adsorbate as a function of the environmental conditions (partial pressure of the adsorbed species and temperature) is described by adsorption isotherms. The most simple is the Langmuir isotherm, which considers only adsorption of the first monolayer. The BET isotherm[1] is applicable also when more than one monolayer is adsorbed and will be used in this article:

$$\frac{V}{V_{\mathrm{mon}}} = \frac{\beta H}{(1 - H)(1 - (1 - \beta)H)} \quad H = \frac{p}{p_0} \tag{1}$$

V and V_{mon} are the total volume of adsorbed material and the volume of one monolayer, respectively. H is the equilibrium vapor pressure above the adsorbed layer p divided by that corresponding to bulk saturation p_0. β is the so-called BET constant which is a function of the enthalpy of desorption from the surface ΔH_{d} and that of evaporation of the bulk liquid ΔH_{vap}:

$$\beta \cong \mathrm{e}^{(\Delta H_{\mathrm{d}} - \Delta H_{\mathrm{vap}})/RT} \tag{2}$$

Here R is the gas constant and T the absolute temperature. If the BET constant is very large, eq 1 can be simplified to

$$\frac{V}{V_{\mathrm{mon}}} = \frac{1}{1 - H} \tag{3}$$

This equation can be used to calculate the relative vapor pressure H in equilibrium with a given amount of adsorbed material.

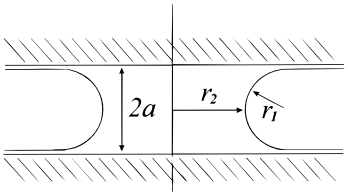

Figure 2. Sketch of a liquid bridge with a, the distance between the solid surfaces, and r_1 and r_2, the two radii of curvature of the liquid bridge.

At the contact point between two particles or a particle and a solid wall, adsorbed layers may join and form a liquid bridge. Liquid bridging is believed to take place at relative vapor pressures higher than a critical one, H_{crit}. It is often stated that H_{crit} is the relative vapor pressure by which the adsorbed layer is so thick that the molecules are sufficiently mobile to form a bridge. If the adsorbate is moisture, many authors (for instance ref 2) quote values for H_{crit} of 65−80%. Coelho and Harnby[3] derived an expression for H_{crit} considering the equilibrium between the bridge and an adsorbed monolayer.

Due to the effects of the gas/liquid and liquid/solid interfaces the surface of a liquid bridge will be net concave (the concave radius of curvature, r_1 is smaller than the convex one, r_2; see the sketch in Figure 2). The exact shape can be calculated from the Young−Laplace equation.[4,5] The surface tension can be thought of as pulling in the concave surface like a stretched membrane, and the pressure in the liquid phase behind the surface is lower than the prevailing pressure:

$$\Delta p = \frac{2\gamma}{r_{\mathrm{m}}} \tag{4}$$

Here r_{m} is the mean radius of curvature[6] (in the situation in Figure 2 equal to $(1/r_1 + 1/r_2)^{-1}$) and γ the surface tension. The lower pressure results in a lower chemical potential of the liquid molecules in the bridge, which gives rise to a lower vapor pressure above the concave surface. This vapor pressure can be calculated from the Kelvin equation:

$$H = \mathrm{e}^{M\gamma/\rho RTr_{\mathrm{m}}} \tag{5}$$

Here M and ρ are the molecular weight and the density of the adsorbate, respectively.

If the circumference of the bridge is not too large compared to the particle dimensions, the force arising from the presence of the liquid bridge has two important contributions:[7] (1) the pressure deficiency force due to the lower pressure in the bridge F_{p}; (2) the surface tension force F_{t}, which is the "pull" due to the surface tension in the bridge surface.

Thus the force is

$$F_{\mathrm{bridge}} = F_{\mathrm{p}} + F_{\mathrm{t}} = A_{\mathrm{bridge}} \frac{\gamma}{r_{\mathrm{m}}} + P_{\mathrm{bridge}}\gamma \tag{6}$$

with A_{bridge} and P_{bridge} the cross-sectional area and the perimeter of the bridge, respectively.

(1) Brunauer, S.; Emmett, P. E.; Teller, E. *J. Am. Chem. Soc.* **1938**, *60*, 309.
(2) Adams, M. J.; Perchard, V. *IChemE Symp. Ser.* **1985**, *42*, 147.
(3) Coelho, M. C.; Harnby, N. *Powder Technol.* **1978**, *20*, 197.
(4) Lian, G.; Thornton, C.; Adams, M. J. *J. Colloid Interface Sci.* **1993**, *161*, 138.
(5) Gao, C. *Appl. Phys. Lett.* **1997**, *71*, 1801.
(6) Israelachvili, J. N. *Intermolecular and surface forces*, 2nd ed.; Academic Press: London, 1992.
(7) Fisher, L. R.; Israelachvili, J. N. *Colloids Surf.* **1981**, *3*, 303.

Due to the particular geometry and periodicity conditions of the system considered in this paper, the developed voids are extended in one direction only, such that the lateral sides are cylindrical of shape. r_2 in Figure 2 is therefore infinite, and we can take the surface of the liquid bridge to be the arc of a circle.[7] r_m, the mean curvature of the surface is then equal to the radius of that circle (r_1 in Figure 2).

Technique of Molecular Dynamics Simulations and Its Application to Modeling Surface/Surface Interaction and Fluid Molecules near Solid Surfaces. In MD simulations[8,9] the classical equations of motion for individual atoms are solved numerically. For atom i

$$m_i \frac{\partial^2 \boldsymbol{r_i}}{\partial t^2} = \boldsymbol{F_i} \quad \boldsymbol{F_i} = -\frac{\partial}{\partial \boldsymbol{r_i}} V(\boldsymbol{r}) \quad i = 1...N \qquad (7)$$

where $\boldsymbol{r}_i$ is the position vector, $\boldsymbol{F}_i$ the force acting on the atom, t time, m_i the mass of the atom, and $V(\boldsymbol{r})$ the potential energy function of the system. Quantum mechanical effects are thus not taken into account explicitly. To save computational effort and since interatomic interactions fall off quickly with distance, the force is often truncated at a given distance from the atom (the cutoff radius).

By the technique of MD, macroscopic properties of complex systems can be described directly in terms of a realistic atomic model. MD simulations are found increasingly useful in giving information, not only about the underlying reasons for the specific properties of existing materials but also about the possibilities for designing new materials with very specific properties.

Some investigations by MD of surface/surface contact and of the structure of liquid water in the vicinity of interfaces have been published. The use of the standard truncations of Coulombic interactions can lead to problems when modeling such nonisotropic and nonhomogeneous systems, particularly when modeling polar liquids such as water. Some investigators have been looking at this issue by comparing different truncation methods with Ewald summation, which takes into account all Coulombic interactions in a periodic way.

Feller et al.[10] investigated the effect of truncating the Coulombic interactions at various radii on the properties of water, both in the bulk and at a vapor interface, by comparing with the Ewald summation. They found that truncation introduced an artificial ordering outside the cutoff leading to a lower self-diffusion coefficient. They also found that truncation introduced a deviation in the surface tension. The discrepancies in the physical parameters caused by truncation were typically around 20%. The Ewald summation was mostly furthest from the experimental values; this was attributed to shortcomings in the TIP3P water model, since the model has been parametrized without Ewald summation.

Shelley and Patey[11] simulated TIP4P water between hydrophobic walls, comparing 2-D Ewald summation with different truncation conventions: minimum image (MI); spherical cutoff (SC); cylindrical cutoff (CC). Among other things, they looked at the density profiles and ordering of the dipole orientations. They found that Ewald summation and SC gave similar results with regular oscillations in the density when moving away from the wall and no ordered dipole orientations in the bulk liquid. MI and CC, on the other hand, showed no ordered density oscillations but an unphysical ordering of the dipoles throughout the liquid. They recommended Ewald summation.

Spohr[12,13] looked at the interfacial electrostatic potential as an indicator for the quality of results. He compared 2-D and 3-D Ewald summation with spherical truncation for systems containing liquid−solid and liquid−gas interfaces. He found that spherical truncation gave unphysical results with small systems. With enough water molecules and a large enough cell (about 60 × 60 Å^2) and cutoff radius, the SC truncation gave acceptable results. He recommends the use of 2-D Ewald summation but finds that many properties, which do not depend strongly on long-range interactions, can be calculated with less computationally demanding techniques.

We mention a few other simulations of systems with interfaces. Schoen and Diestler[14] studied the properties of thin films of Lennard-Jones fluids confined to a slit-shaped pore, essentially two opposing plane-parallel solid walls, by Monte Carlo. They studied walls that were partly strongly adsorbing and partly weakly adsorbing in a striped pattern. This particular configuration resulted in liquid bridging when the walls were sufficiently close together and when the interaction between the Lennard-Jones particles and the walls was strong enough. Using the same simulation technique, Schoen[15] studied the stress−strain behavior of a monolayer film confined between two solid surfaces while shearing the walls.

Lee and Rossky[16] investigated the structure of liquid water near three different types of solid surfaces. They found that the perturbation of the water due to the adsorption on the surface did not exceed a distance of 10 Å from the surface. They also found that the density perturbation was stronger near a hydrophilic surface (silica) with a peak number concentration of atoms of 1.5−1.7 times the bulk value in the first monolayer.

Webb and Garofalini[17] investigated the approach and withdrawal of crystalline metal to a glass surface by MD techniques. They studied the states of stress in the materials resulting from the contact and the effect in bringing about crystalline defects.

Thompson and Robbins[18] studied the angle of interfacial contact between two immiscible liquids on a solid during shear. Molecular interactions were modeled as a Lennard-Jones interaction potential with a cutoff radius. They found that the no-slip condition, normally applied in macroscopic fluid dynamics, broke down in the first monolayers. D'Ortona et al.[19] looked at the spreading of a droplet of organic liquid on a solid surface. They also calculated intermolecular forces with a Lennard-Jones potential using a cutoff radius. To take into account long-range interactions between liquid molecules and solid, they included a long-range van der Waals potential. They observed "terraced" spreading in well-defined monolayers. They found that the long-range potential did not make much difference to the results.

Experimental Investigations of Interparticle Interaction without and with Adsorbed Agents

(8) Allan, M. P.; Tildesly, D. J. *Computer simulation of liquids*; Oxford University Press: Oxford, U.K., 1987.
(9) Van Gunsteren, W. F.; Berendsen, H. J. C. *Angew. Chem., Int. Ed. Engl.* **1990**, *29*, 992.
(10) Feller, S. E.; Pastor, R. W.; Rojnuckarin, A.; Bogusz, S.; Brooks, B. R. *J. Phys. Chem.* **1996**, *100*, 17011.
(11) Shelley, J. C.; Patey, G. N. *Mol. Phys.* **1996**, *88*, 385.
(12) Spohr, E. *J. Chem. Phys.* **1997**, *106*, 388.
(13) Spohr, E. *J. Chem. Phys.* **1997**, *107*, 6342.
(14) Schoen, M.; Diestler, D. J. *Phys. Rev. E* **1997**, *56*, 4427.
(15) Schoen, M. *Physica A* **1997**, *240*, 328.
(16) Lee, S. H.; Rossky, P. J. *J. Chem. Phys.* **1994**, *100*, 3334.
(17) Webb, E. B.; Garofalini, S. H. *J. Chem. Phys.* **1994**, *101*, 10101.
(18) Thompson, P. A.; Robbins, M. O. *Phys. Rev. Lett.* **1989**, *63*, 766.
(19) D'Ortona, U.; De Coninck, J.; Koplik, J.; Banavar, J. R. *Phys. Rev. E* **1996**, *53*, 562.

Present. Two important techniques for measuring the interaction between surfaces on a microscopic level have emerged: the "surface force apparatus" (SFA) and atomic force microscropy (AFM).

The latter is based on approaching a tip of an AFM cantilever to a surface, monitoring the force acting on the tip as a function of the surface separation. Jarvis et al.[20,21] avoided the proximity limitation normally dictated by the "jump to contact" distance by applying a restoring force to the cantilever. Landman et al.[22] avoided the same problem by always choosing a cantilever so stiff that jump-to-contact did not occur; they also supported their experiments with molecular dynamics simulations. AFM is often applied under conditions of ultrahigh vacuum or under liquid in order to avoid the disturbing effects of adsorbed species on the surfaces. The present authors are not aware of any studies of the effect of adsorbed species on surface−surface interaction using this technique.

In the SFA, on the other hand, the effect of adsorbed species on the interaction between surfaces has been looked at in some detail.[6,7] Fisher and Israelachvili[7] determined the interaction between molecularly smooth mica surfaces in atmospheres of cyclohexane and water vapor at varying relative pressures. They compared the measured forces with macroscopic bridging theory as represented by eqs 4−6. They found that with cyclohexane the measured forces agreed with the theoretical ones down to the very low relative vapor pressure of 0.1, corresponding to absolute values for r_m of around 0.5 nm, which is of molecular dimensions.

With water vapor the measured force became lower than the theoretical one already from high ($H > 0.95$) relative vapor pressures, corresponding to an absolute value of r_m of about 10 nm. The order of magnitude of the measured force, however, remained in rough agreement with macroscopic theory, the measured force being some $^2/_3$ of the theoretical one for $H \cong 0.6$, corresponding to $|r_m| \cong 1$ nm.

Objective of the Present Investigation. The objective of this investigation was to explore the potential of MD simulations for the investigation of the effect of adsorbed species on particle/particle and particle/wall interactions. The method of doing this was to create two opposing solid crystal surfaces with a number of water molecules between, allowing the water molecules to move freely under the influence of the forces acting on them. The system would then be studied at various surface separations, both with respect to the nature and morphology of the adsorbed water and the forces acting between the surfaces.

Method

The MD simulations were performed with the software package GROMACS (GROningen MAchine for Chemical Simulations), which was developed in the Department of Biophysical Chemistry at the University of Groningen.[23] Periodic boundary conditions were used. The present application of the software is atypical in a number of ways. For this reason a considerable effort had to be expended in generating a suitable starting structure (see below for the details). One issue, which had to be addressed, was whether the use of a spherical cutoff radius was suitable also in the present highly nonhomogeneous and nonisotropic system.

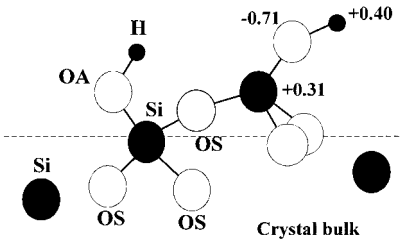

Figure 3. Details of the crystal surface with the bonds indicated. In the left of the two tetrahedrons the different atom labels as used in the GROMOS/GROMACS force field are indicated; in the right one the atomic charges different from zero are indicated. The bold oxygen is used to define the distance between the two crystal surfaces.

In other words: does the bulk crystal beyond the cutoff radius contribute significantly to the water molecule/crystal interaction? To ascertain this, a special "background potential" or "crystal bulk correction" (CBC) was developed to account for interactions between the molecules of the adsorbate and the part of the crystal bulk outside the cutoff radius.

Generating the Starting Structure. The initial idea was to use glass as the solid. However, the generation of glass, with its amorphous polymeric structure, would have been too difficult, with probably only little improvement over a system built from a more simple solid with a regular crystal lattice: α-quartz.

The coordinates of α-quartz were obtained from the library of the molecular modeling program Cerius. The unit cell was then transformed to one with the (1,0,−1) Miller plane as one surface.[24] This unit cell was then multiplied in space to create a crystal of the required thickness (more than one cutoff distance, $R_c = 1.2$ nm). The crystal was then rotated to make the (1,0,−1) Miller plane coincide with the *x*,*y*-plane after which silanol groups were created by adding hydrogen atoms to the surface oxygen atoms and generating the necessary bonds.

For water the SPC (single point charge) model[25] was used. This model consists of two positive charges (+0.41 e) at the hydrogen positions and one negative (−0.82 e) at the oxygen position, the latter carrying a Lennard-Jones repulsion and attraction term. The bond length is 0.1 nm, and the bond angle, 109.47°. A layer of SPC water was taken from an equilibrated simulation and built in 0.4 nm above the crystal surface (to avoid initial "bad" crystal−water interactions). The entire structure was mirrored to create the opposing surface. The water layers were energy minimized by the method of steepest descent, whereafter the system was equilibrated by performing a 10 × 10 ps simulation with generation of velocities according to a Maxwellian distribution at the beginning of every 10 ps of simulation.

To simulate infinitely large crystal slabs, periodic boundary conditions were used, so that an atom at the edge of the computational cell had interactions with those of its periodic neighbors falling within its spherical cutoff radius. To mimic 2-D periodic boundary conditions, a void was used at both top and bottom (*z*-axis) of the simulation cell (see also ref 10).

To the GROMACS software, the crystals appear as infinitely large molecules. To avoid using unnecessary computer time the atoms internal to the crystals were fixed in space. Their mutual force fields were calculated. Only the atoms at the crystal surfaces were provided with their appropriate bonds and dihedrals and allowed to move. Figure 3 shows a detail of the crystal surface with the bonds indicated. The charge distribution on the surface atoms was taken from literature.[16] Figure 4 shows a complete starting structure. Note that the water molecules are represented with staffs and not with their van der Waal's dimensions. Table 1 gives an overview of the atoms used in the starting structure with their Lennard-Jones force-field parameters and charges. The combination rule for Lennard-Jones interactions between different atoms was taken to be the geometric mean.

(20) Jarvis, S. P.; Yamada, H.; Yamamoto, S. I.; Tokumoto, H.; Pethica, J. B. *Nature* **1996**, *384*, 247.
(21) Jarvis, S. P.; Yamamoto, S. I.; Yamada, H.; Tokumoto, H.; Pethica, J. B. *Appl. Phys. Lett.* **1996**, *70*, 2238.
(22) Landman, U.; Luedtke, W. D.; Burnham, N. A.; Colton, R. J. *Science* **1990**, *248*, 454.
(23) Berendsen, H. J. C.; van der Spoel, D.; van Drunen, R. *Comput. Phys. Commun.* **1995**, *91*, 43.
(24) Janossy, I.; Menyhard, M. *Surf. Sci.* **1971**, *25*, 647.
(25) Berendsen H. J. C.; Postma, J. P. M.; van Gunsteren, W. F.; Hermans, J. In *Intermolecular forces*; Pullman, B., Ed.; Reidel: Dordrecht, The Netherlands, 1981; p 331.

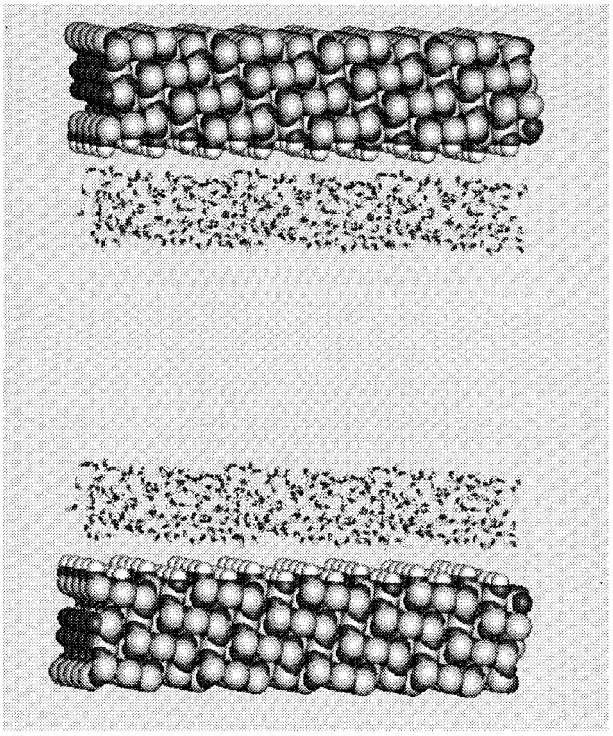

Figure 4. Complete starting structure. The dimensions of the crystals are 5.49 × 4.91 × 1.45 nm. Distance between the crystals: 6 nm.

Table 1. Different Types of Atoms and Their Force-Field Parameters

atom type	label	$C^{(6)}$ [a] (kJ nm^{12} mol^{-1})	$C^{(12)}$ [a] (kJ nm^{6} mol^{-1})	q (e)
hydrogen (surface)	H			+0.40
hydrogen (SPC)	H			+0.41
oxygen (crystal)	OS	0.22617×10^{-2}	0.74158×10^{-6}	
oxygen (surface)	OA	0.22617×10^{-2}	0.15062×10^{-5}	−0.71
oxygen (SPC)	OW	0.26177×10^{-2}	0.26331×10^{-5}	−0.82
silica (crystal)	SI	0.22617×10^{-2}	0.22191×10^{-4}	
silica (surface)	SI	0.22617×10^{-2}	0.22191×10^{-4}	+0.31

[a] $C^{(6)}$ and $C^{(12)}$ for pairs of different atoms I and J were calculated using the geometric mean of the atomic values of I and J.

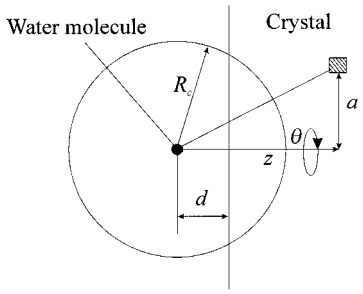

Figure 5. Sketch explaining the calculation of the crystal bulk correction term.

Background Potential or Crystal Bulk Correction (CBC). Although the cutoff radius of 1.2 nm usually has a negligible effect on MD results obtained for isotropic molecular systems without explicit charges, the present system is so highly nonisotropic that it was decided to include a crystal bulk half spaces correction term to account for the effect on the adsorbed molecules of the crystal bulk outside the cutoff radius. Since the crystal bulk is electroneutral, the long-range Coulombic interactions between water and the crystal bulk are expected to be negligible as a good approximation. The dispersion terms, however, are always attractive, and for the contribution to the CBC, we have to integrate the energy density,

$$w(z,a,\theta) = \frac{C_{12}}{(a^2+z^2)^6} - \frac{C_6}{(a^2+z^2)^3} \tag{8}$$

over the half space of the crystal, where C_{12} and C_6 are Lennard-Jones interaction parameters between the oxygen atom of a water molecule and a volume element in the crystal (see for definitions of the symbols also eq 11 below and Figure 5).

For a water molecule further away from the crystal than the cutoff radius, R_c, an integration over the crystal gives the total potential for a molecule a distance d away from the surface:[6]

$$w(d) = \int_d^\infty \mathrm{d}z \int_0^{2\pi} \mathrm{d}\theta \int_0^\infty a\ \mathrm{d}a \left[\frac{C_{12}}{(a^2+z^2)^6} - \frac{C_6}{(a^2+z^2)^3}\right] = \frac{\pi C_{12}}{45 d^9} - \frac{\pi C_6}{2 d^3} \tag{9}$$

For this reason, this type of surface is sometimes referred to as a "9−3 Lennard-Jones wall" and was used, e.g., by Lee and Rossky,[16] Shelley and Patey,[11] and Schoen and Diestler.[26]

For a water molecule where $d < R_c$, such as sketched in Figure 5, the potential has to be corrected by subtracting the potential due to the portion of crystal falling within the cutoff, which is being accounted for in the normal way by the direct calculation of the interatomic interactions.

The result is

$$w(d) = \frac{\pi C_{12}}{45 d^9} - \frac{\pi C_6}{6 d^3} \quad d > R_c$$

$$w(d) = \pi C_{12}\left[\frac{2}{9 R_c^{\,9}} - \frac{d}{5 R_c^{\,10}}\right] - \pi C_6\left[\frac{2}{3 R_c^{\,3}} - \frac{d}{2 R_c^{\,4}}\right] \quad d \le R_c \tag{10}$$

The fact that in our system the crystals contain different kinds of atoms can be accounted for by defining the C_{12} and C_6 parameters as the sum of contributions arising from atoms of type J to the force on the Ith type:

$$C_{12} = \rho_N \sum_J x_J C_{IJ}^{(12)}$$

$$C_6 = \rho_N \sum_J x_J C_{IJ}^{(6)} \tag{11}$$

Here ρ_N is the number density of atoms in the crystal, x_J the mole fraction of type J, and $C_{IJ}^{(6)}$ and $C_{IJ}^{(12)}$ are the Lennard-Jones parameters between individual atoms of type I and J.

Simulations. Several simulations of 400 ps have been performed at 300 K, using a time step of 2 fs and a cutoff radius R_c of 1.2 nm, with different numbers of water molecules (up to 1500 in total, 750 per crystal surface) and different surface separations. All bond lengths were fixed using SHAKE.[27]

The temperature was controlled by the method of weak coupling to a thermostat[28] with a reference temperature of 300 K and a time constant of 0.4 ps.

Analysis of Diffusion. Diffusion constants were determined using the Einstein relation from a plot of the mean square displacement versus time. Local diffusion constants were determined by assigning atoms to their positions at $t = 0$ and limiting the analysis to a time interval from 0 to 5 ps. The axial and planar diffusivities were distinguished and calculated from the equations

$$2D_z t = \langle(\Delta z)^2\rangle \tag{12}$$

$$4D_{pl} t = \langle(\Delta x)^2\rangle + \langle(\Delta y)^2\rangle \tag{13}$$

respectively. Δx and Δy are the path lengths during t in the two

(26) Schoen, M.; Diestler, D. J. *Chem. Phys. Lett.* **1997**, *270*, 339.
(27) Ryckaert, J.; Ciccotti, G.; Berendsen, H. J. C. *J. Comput. Phys. Commun.* **1977**, *55*, 13.
(28) Berendsen, H. J. C.; Postma, J. P. M.; van Gunsteren, W. F.; Di Nola, A.; Haak, J. R. *J. Chem. Phys.* **1984**, *81*, 3684.

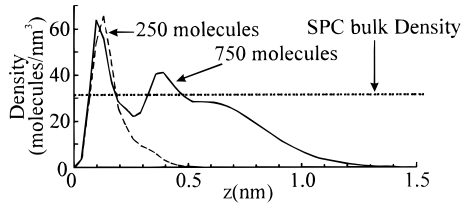

Figure 6. Density profiles in the adsorbed layers at a crystal surface separation of 6.0 nm.

coordinate directions in the plane of the crystal surface and Δz is the path length in the direction of the transverse coordinate.

Results and Discussion

Large Surface Separations. To study the nature of the adsorbed layers under conditions where the two plates and their adsorbed water molecules are outside each other's range of influence, simulations were performed at surface separations of 6 nm. Figure 6 shows some of the obtained density profiles. If one takes 3.55 Å as the equilibrium molecular separation for water and assumes hexagonal close-packing of the adsorbed molecules, 750 molecules per crystal corresponds to an adsorbed layer thickness of 3.05 monolayers, corresponding to a value for H of 67% according to the (simplified) BET isotherm, eq 3. A rough estimate for β for this system is 154 (so $\beta \gg 1$).

The density profiles clearly show a highly ordered layer packing of the water molecules close to the crystal surface, in the case of 750 molecules in at least two distinct layers. To determine the extent to which the water molecules were oriented, an order parameter (average orientation of water dipoles with respect to the z-axis) was evaluated. Its value was roughly the same as for polar−apolar, liquid−liquid interfaces such as water−decane. This means that scarcely any orientation in the dipoles could be distinguished. This indicates that the water behavior was in accordance with ref 11. We note that in ref 11 the walls used were hydrophobic, but according to ref 29 the fact that our walls are hydrophilic should not lead to more ordering, rather less: at a hydrophobic interface the hydrogen-bonding network is being disturbed, yielding an extra ordering of water molecules to compensate for the loss of hydrogen bonds, whereas with the present hydrophilic surface water molecules can form hydrogen bonds more or less like in the liquid bulk. The spherical cutoff radius of 1.2 nm used here is held by Spohr[13] to give some problems as far as the electrostatic potential of interfaces is concerned; he recommends using 2-D Ewald summation to avoid this. Our software does not allow 2-D Ewald summation. However, Spohr also states that the density, diffusivity, and dipole distribution, which are important in this study, are not affected much by the boundary conditions and that among the other alternatives the spherical cutoff (used by us) gives results closest to the 2-D Ewald results.

The peak density in the first layer exceeds twice the density of bulk SPC water and thus exceeds that found by Lee and Rossky.[16] The density decreases to zero toward the surface. Although the surface of the adsorbed layer was quite distinct, it was always slightly undulating causing the gradual decrease of the density profile near the surface.

(29) van Buuren, A. R.; Marrink, S. J.; Berendsen, H. J. C. *J. Phys. Chem.* **1993**, *97*, 9206.

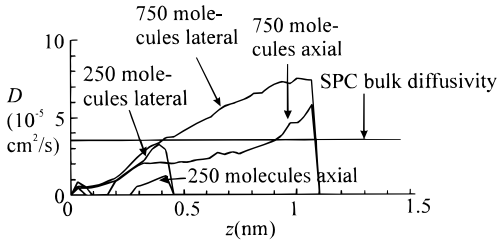

Figure 7. Profiles of molecular diffusivity in the adsorbed layers at a crystal surface separation of 6.0 nm.

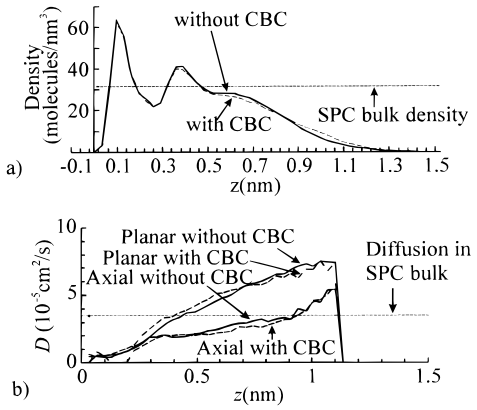

Figure 8. (a, b) Density and diffusion profiles in the adsorbed layer, with and without the CBC included. Crystal surface separation: 6.0 nm, with 750 molecules/crystal.

The density of the first adsorbed layer is much the same for the two situations shown in Figure 6, so that the nature of the first layer is not significantly affected by the presence of further layers on top of it.

The molecular diffusivity was split up in axial and planar components. Figure 7 shows these plotted against distance from the crystal surface for a surface separation of 6 nm. As one might intuitively expect, the axial mobility is considerably less than the planar one. The mobility can be seen to increase with increasing distance from the crystal surface from considerably less to considerably more than the mobility in bulk SPC−water. The equations for the diffusivity (eqs 12 and 13) are only valid if the particle can move freely within the period it is being tracked, and it is not subject to any strong gradients in free energy. In the present case, the particle center of gravity did not move much within the 5 ps period of tracking, and it is our experience from other work that the external forces were not sufficient to cause errors.

Effect of the Background Potential. Electrostatic interactions between the water molecules and the bulk crystal will, despite them being long-range interactions, cancel at longer separations, since the crystal is electrically neutral. The dispersion forces are short-range but will not cancel in the same way, since they are all attractive. We therefore found it interesting to check the effect of the CBC.

In the present system the bulk correction potential turned out to have very little effect on the results. Figure 8a,b shows the density and diffusion profiles in the adsorbed layers with and without the background potential included. Calculating the molecular interactions within the standard cutoff distance appears to be sufficient for structural and dynamic properties of the water layers, with the exception of long-range electrostatic interactions, which should be treated with 2-D Ewald summation as mentioned.

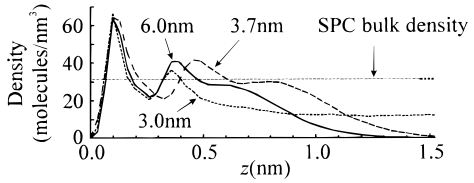

Figure 9. Density profiles in the adsorbed layers for different surface separations with 750 molecules/crystal. The constant limiting density at 3.0 nm separation is due to bridge formation (the density was determined from the total number of molecules in a slice perpendicular to the z-direction).

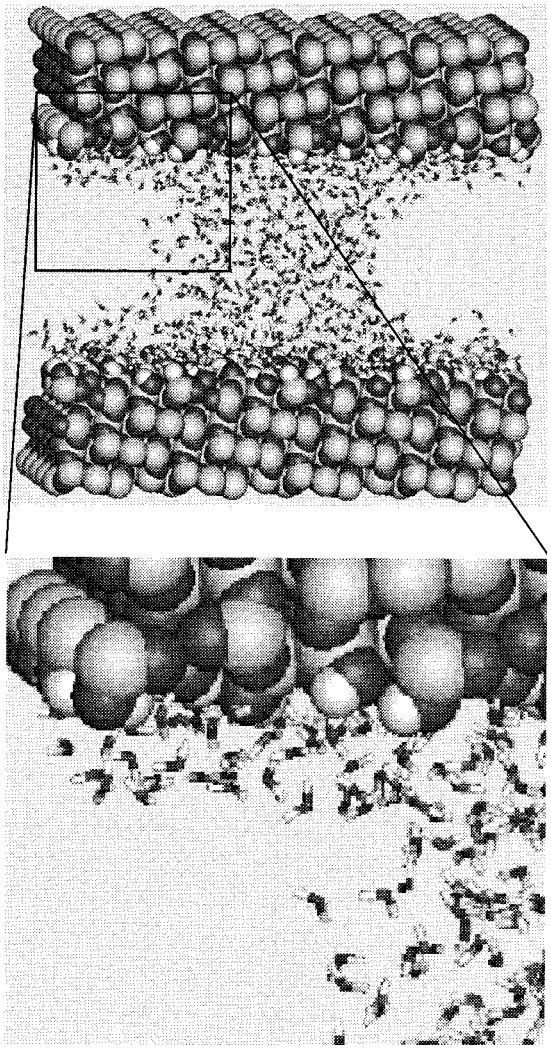

Figure 10. Snapshot of an end configuration with a surface separation of 3.0 nm and 750 molecules/crystal.

Bringing the Surfaces Closer Together. Figure 9 shows the density profiles at three different surface separations. At a separation of 3.7 nm, the two plates with their adsorbates are coming within the range of mutual influence, and the adsorbed layers are becoming less dense than they were at 6.0 nm, although the density profiles remain qualitatively the same. At a surface separation of 3.0 nm the density profile changes fundamentally.

The reason for this can be seen in the snapshot shown in Figure 10. The adsorbed layers have joined in a bridge. The radius of curvature of the bridge can be seen to be around 1.1 nm. Some adsorbed material (a couple of monolayers) remains on the surface, showing that the situation is one of equilibrium between adsorption and bridge formation. This will be discussed further below.

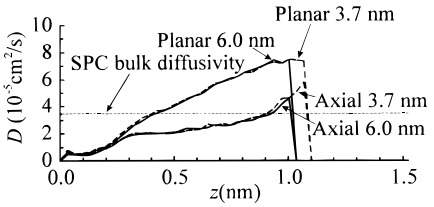

Figure 11. Molecular diffusivity in the adsorbed layers at two different surface separations with 750 molecules/crystal.

The bridge formation already appears within the first 20 ps of the simulation and remains stable during the rest of the simulation time. Note that the cavity has a cylindrical shape. Under the constraints of the periodic boundary conditions, this geometry leads to the minimal surface area for the case shown.

Figure 11 shows the molecular mobility in the layers at surface separations of 6.0 and 3.7 nm. It is clear that the mobility is not significantly affected by the proximity of the two surfaces.

Further Discussion

The simulation is at any given surface separation a closed system at constant volume. For an understanding of the analysis it is important to realize that, as long as the volume available to the water molecules exceeds the volume required by the dense phase, the system in principle contains two fluid phases in equilibrium: an adsorbed liquidlike one and a gaseous one. Most of the time no gaseous water molecules are observed since the total volume available to the gas is only a fraction of the volume taken up by a single gaseous molecule under the simulation conditions; the "gas phase" therefore consists of a molecule escaping the adsorbed layers once in a while. The fact that the system contains two phases means that there is one degree of freedom less than in systems normally encountered in the literature which contain only one phase. Therefore the densities of the adsorbed and the gas phases are meaningful physical parameters, which are established spontaneously and reach equilibrium values despite the system being closed. It can be argued that the μVT ensemble is a more natural choice for these simulations than the NVT ensemble used. However, since we are dealing with a two-phase system, a valid equilibrium corresponding to a unique relative humidity H will be established also in our NVT system, which involved less simulation time, since convergence in the NVT ensemble is expected to be faster than in μVT. The relative humidity H will be determined by our choice of N, the number of molecules, rather than μ.

The crystal surfaces are hydrophilic,[16] so the water/surface "contact angle" should be zero. In the present two-phase equilibrium system we would expect at least one adsorbed monolayer to be present at all conditions of practical interest. If the plates had been less hydrophilic and/or less water molecules were present in the system, we could expect part of the solid surface to be free of water molecules and would expect quite a different behavior, with different bridge shapes. This is an interesting subject for further research. According to the BET isotherm (eq 3), a bit more than three monolayers in the present system corresponds to a relative vapor pressure (or relative humidity) H of 67%. If equilibrium conditions are maintained in the system, bridge formation should take place at the surface separation when bridging becomes energetically advantageous, and the resulting bridge curvature should correspond to about the same H as the adsorbed layer thickness. On the other hand, bridge formation is

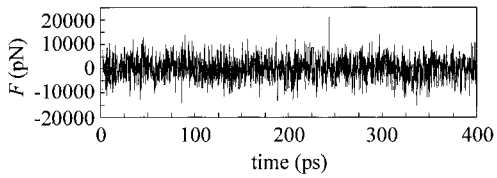

Figure 12. Plot of instantaneous values for the force acting on a crystal as a function of time. Surface separation: 3.7 nm, with 750 molecules/crystal.

probably subject to nonequilibrium effects: the adsorbed water layers will—in a physical system, and particularly in the present system where a cutoff radius R_c is used—not join in a bridge until they are within the range of mutual influence, and there will be a hysteresis effect in bridge formation and breakage.

In any case, once a bridge is formed, equilibrium between the molecules in the bridge and those in the adsorbed layers remaining on the crystal surface (clearly visible in Figure 10) should prevail, reflecting the competition between the low pressure in the bridge on one hand and proximity to the solid surface on the other. In line with the experimental investigation of Fisher and Israelachvili,[7] we can compare our results, in terms of order of magnitude, with the predictions of macroscopic thermodynamics. The thickness of the remaining adsorbed layers appears to be a couple of monolayers (see Figures 9 and 10), corresponding to H of about 50% according to eq 1. The bridge curvature, on the other hand, in Figure 10 is about 1.1 nm, and this would, according to the Kelvin eq 5, using the macroscopic value for the surface tension of water, correspond to a relative humidity of 62%. If one takes into account the uncertainties involved, these rough calculations show that the observed phenomena are consistent with what one would expect. Note that bridge formation with other thicknesses of the adsorbed layers has not yet been studied, and neither has the effect of changing the cutoff radius.

The total force acting on the crystals was evaluated as the sum of all forces acting on the individual crystal atoms. This calculation was complicated by very strong fluctuation in the instantaneous values due to motion of the individual molecules. In fact, the standard deviation of the block-averaged force (that is, determined by grouping the data in blocks and using standard statistics on the block averages, see ref 8) was always at least 1 order of magnitude greater than the mean value. This made simulation over long periods (400 ps) necessary before a statistically significant result for the mean force—the spread in which is proportional to the reciprocal of the square root of the number of simulation steps—could be obtained. The reasons for this fluctuation in the force have not been established unequivocally. A possible explanation is dipole−dipole interactions being broken and established as water molecules move in and out of the 1.2 nm Coulombic cutoff distance from the crystal surface; however, even with water layers thinner than the cutoff radius, the fluctuation was undiminished. Figure 12 shows a typical plot of the instantaneous force against simulation time.

The forces calculated are shown in Table 2. At the surface separations of 6.0 and 3.7 nm, no statistically significant force between the crystals can be detected. At the surface separation of 3.0 nm, where bridging occurs, the attractive force between the surfaces of 1260 pN is clearly statistically significant. For comparison, the expected force was calculated from eq 6 using the macroscopic surface tension of water and the bridge curvature of 1.1 nm as r_m. Both the pressure deficiency force (calculated at the neck) and the surface tension force contributed about 700 pN, giving $F_{bridge} \cong 1400$ pN. Clearly the comparison is reasonable, again confirming that the phenomena observed are physically realistic ones. The statistical significance is not high enough to make any detailed comparisons such as those made by Fisher and Israelachvili[7] for their experimental results.

Table 2. Time-Averaged Forces (in pN = 10^{-12} N) Acting on the Crystals[a]

surface separation (nm)	F_1 (pN)	F_2 (pN)	$\langle F \rangle$ (pN)
	250 Molecules/Crystal		
6.0	24 ± 480	−90 ± 540	27 ± 360
	750 Molecules/Crystal		
6.0	210 ± 640	75 ± 730	86 ± 480
3.7	150 ± 750	−32 ± 570	73 ± 450
3.0	1270 ± 620	−1250 ± 600	1260 ± 430

[a] The spreads are one standard deviation for the averages shown. F_1 and F_2 are the forces acting on the individual crystals.

Extension of these results to the calculation of real forces between particles is not as far away as one might think. The sort of bridging observed here is likely to be taking place at the periphery of a particle/particle or particle/wall contact point, giving rise to attractive forces. In the center of a contact, on the other hand, compression is likely to prevail, squeezing some of the molecules out (the high pressure giving a high chemical potential causing molecules to move out of the region), while others may remain between the solid surfaces (the lowering of the chemical potential due to proximity to the particle surface canceling the effect of the high pressure). If the surface separation is varied in the sort of simulations shown in this article, all these phenomena can be more or less directly studied, without the need for going to much larger scale. Comparison of simulation results with actual experimentally determined particle/particle and particle wall interactions would then only depend on obtaining sufficient information about the surface morphology on a microscale.

List of Symbols

a	1/2 surface/surface distance
A	cross-sectional area
C_6	attractive parameter of CBC potential for type I
$C_{IJ}^{(6)}$	attractive parameter of Lennard-Jones potential between types I and J
C_{12}	repulsive parameter of CBC potential for type I
$C_{IJ}^{(12)}$	repulsive parameter of Lennard-Jones potential between types I and J
d	atom/surface distance
D_{pl}, D_z	diffusivity in and normal to the plane of the crystal surface, respectively
F	average force per unit area perpendicular to the surface
F_p	pressure deficiency force
F_t	surface tension force
$\boldsymbol{F_i}$	vector force acting on the ith atomic particle
H	vapor pressure divided by the saturation vapor pressure
H_{crit}	relative vapor pressure at which bridge formation sets in
ΔH_d	enthalpy of desorption
ΔH_{vap}	enthalpy of vaporization
m_i	mass of molecule i

M	molecular mass
p	(vapor) pressure
p_o	saturation (vapor) pressure
P	perimeter
R	gas constant
r_m	mean curvature of bridge surface
$\mathbf{r_i}$	positional vector of the ith atomic particle
T	temperature
V	volume
V_{mon}	volume of one adsorbed monolayer
w	potential
x, y, z	Cartesian coordinates
x_I	mole fraction of atom type I

Greek Letter

β	BET constant
γ	surface tension
μ	chemical potential
ρ	density
ρ_N	number density of atoms

Acknowledgment. The authors thank Dr. ir. David van der Spoel and Dr. Peter Tieleman for help with the software and Dr. Frank Everdij for setting up the density analysis. They have all helped us with valuable discussions.

LA000009E